EKOLOGIJA. 2010. Vol. 56. No. 3–4. P. 144–152
DOI: 10.2478/v10055-010-0020-x

Mapping total nitrogen in ash after a wildland fire: a microplot analysis

Paulo Pereira[1, 2*],

Xavier Úbeda[1],

Edita Baltrėnaitė[2]

[1, 2] *Environmental Research Group, Department of Physical Geography and Geographic Regional Analysis, Montalegre 6, University of Barcelona, Catalunya, Spain*

[2] *Department of Environmental Protection, Vilnius Gediminas Technical University, Saulėtekio Ave. 11, LT-10223 Vilnius, Lithuania*

Nitrogen (N), due its low temperature volatilization, is one of the elements most vulnerable to fire. This effect depends on fire severity, which varies depending on biophysical conditions which can be heterogeneous across the landscape. Hence, fire effects on N can be variable. The aim of this study was to establish the ash total nitrogen (TN) spatial variability in a microplot designed in a burned area, and to test several methods in order to identify the most accurate one for interpolating the variable. In total, we selected four deterministic interpolation methods – inverse distance to a weight (IDW), with the weight of 1, 2, 3, 4 and 5, local polynomial (LP), with the power of 1 and 2, global polynomial (GP), radial basis functions (RBF) – spline with tension (SPT), completely regularized spline (CRS), multiquadratic (MTQ), inverse multiquadratic (IMTQ) and thin plate spline (TPS) – and two geostatistical methods: ordinary kriging (OK) and simple kriging (SK). In total, we tested 15 techniques. Ash TN was negatively related to fire severity showed a good spatial structure across the plot. The linear model was the best, which means that the variability of ash TN content increased in all the area of interest. The highest concentration of TN was observed in the northeast part of the plot and the lowest in the Southwest. From all test methods, MTQ was most accurate, and IDW5 was the worst predictor. In general, RBF and the geostatistical methods were most precise and IDW was less accurate, which means that ash TN distribution has some specific features and does not exhibit a small-scale variation. The distribution of the variable depends on species distribution, temperature and probably on vegetation moisture during fire evolution.

Key words: fire severity, biophysical conditions, ash total nitrogen, microplot, interpolation methods

INTRODUCTION

Wildland fires affect enormous extensions of forests. In a great majority, they result from anthropogenic activities leading to serious problems of land degradation and desertification. Nevertheless, fire is a natural element of the ecosystems. From the savannas, where fire has an annual frequency, to the taigas where fires can have a century of recurrence, fire has shaped all earth biomes (Mataix-Solera, Cerdà, 2009). The most visible thing after a fire is ash, and this residue contains the majority of the nutrients available for ecosystem recovery. The amount and type of nutrients depend on the temperature reached, species affected and contact time (Pereira et al., 2009a, 2010). Nitrogen (N) is the most limiting element in wildland ecosystems (Neary et al., 2005), thus requiring special attention when managing fire. Also, N is one of the most vulnerable elements to fire volatilization. N volatilization starts at temperatures of ±200 °C, and at temperatures above 500 °C all N is completely vaporized (DeBano et al., 1998; Neary et al., 2005). During fires, temperatures could reach 900 °C in soil surface and litter, hence the probability of wildfire impact on N pools and biogeochemical cycles is very high (DeBano, 1981).

Biophysical conditions (plant composition, distribution and moisture, the amount of biomass, topography, vegetation moisture, meteorological conditions) vary across the landscape. These characteristics influence the fire behaviour and effects. The different characteristics of the area affected by fire induce a complex and heterogeneous mosaic of fire impacts (Viegas, 2004; Crimmins, 2005; Baeza et al., 2006; Maingi, Henry, 2007).

* Corresponding author. E-mail: pereiraub@gmail.com

Recently, some studies have reported that the effects of fire on nutrient status across small distances can be highly variable due to the effects of microtopography and vegetation characteristics (Lorca, Úbeda, 2004; Úbeda et al., 2005; Pereira, Úbeda, 2010). This adds a great complexity to understanding the effects of forest fires on the landscape. The high spatial variability induces serious difficulties while estimating the correctly values at unsampled points. This estimation is achieved by testing diverse interpolation methods. However, the great availability of methods imposes a challenge but also offers an opportunity to elucidate the best method for interpolating surfaces. The interpolation accuracy is assessed by the cross-validation method widely used in similar studies (Zhang, McGrath, 2004; Diodato, Ceccarelli, 2005; Bourennane et al., 2006; Pereira, Úbeda, 2010).

Several studies have noted that different methods can be more appropriate depending on the distribution of the variable, plot design and the distance between sampling points (Erxleben et al., 2002; Robinson, Metternicht, 2006; Bourennane et al., 2006; Chaplot et al., 2006). A good prediction of the variable allows a better understanding the effects fire on the landscape.

The aim and goal of this study were the distribution and variability of ash total nitrogen (TN), on a microplot scale, of ash collected in a wildfire which occurred in Portugal. To evaluate the performance of the interpolation, we tested 15 interpolation techniques to identify the most accurate one for predicting TN in the ash produced after a wildfire.

DATA AND METHODOLOGY

Study site, sample collection and laboratory analysis

The wildfire occurred in Peninsula de Setubal, near Lisbon region, and affected ±4 ha of a forest dominated by *Quercus suber* and *Pinus pinaster* (Fig. 1). The wildfire sprouted from East to West. Inside this area, we designed a 6 × 13 m microplot (Fig. 2) and collected 30 ash samples. The coordinates of each sampling point were taken with the GPS. Ash samples were collected in soil surface, stored in plastic bags and taken to laboratory. One gram of ash had been pulverized for two minutes on a Fritch pulverisette 23 before analysis. TN was analyzed by the process of combustion-reduction in gas chromatography with the EA Flash Series 112 detector of thermic conductivity (Thermo-Fisher Scientific, Milan). The data acquisition and the respective calculus were effectuated with the Eafer 300 software (Thermo-Fisher Scientific, Milan). The results are presented as a percentage of a dry sample. Fire severity was assessed by checking the ash colour by the Munsell colour chart (Munsell, 1975) and by ash $CaCO_3$ content. A detailed description of the methodology is presented elsewhere (Úbeda et al., 2009).

Statistical analysis

Some basic statistical data were collected, such as the mean (m), standard deviation (SD), the coefficient of variation

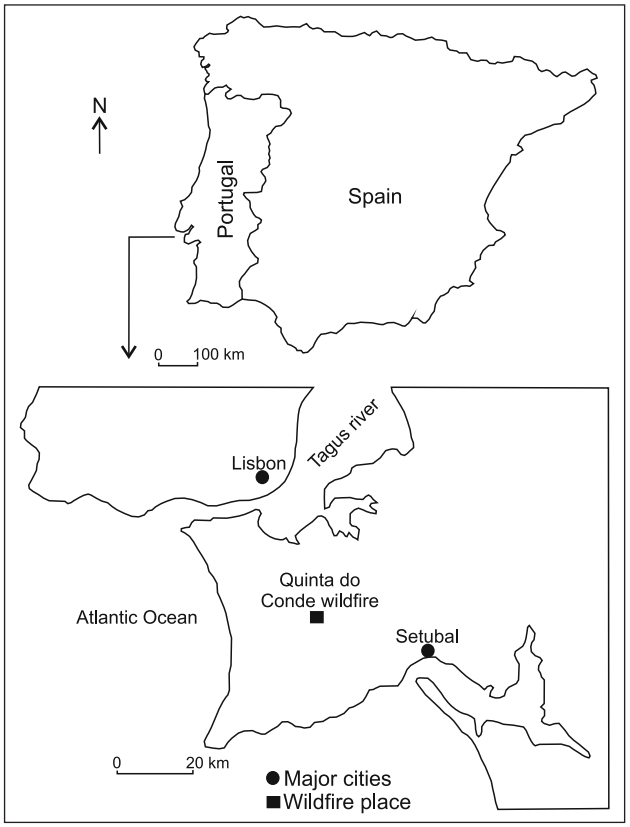

Fig. 1. Study area

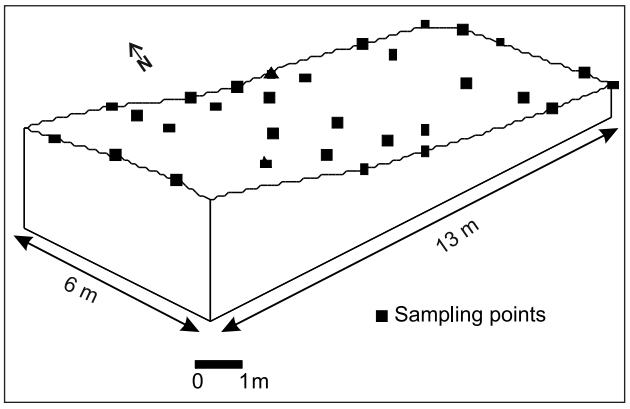

Fig. 2. Plot design and sample distribution

(CV(%)), minimum (min) 1st quartil (Q1), median (M), 3rd quartil (Q3), maximum (max), skewness (SK) and kurtosis (Kur). The Pearson correlation coefficient was analyzed for fire severity by checking ash colour in the Munsell colour chart, with the chroma value (CV), and the $CaCO_3$ content (Pereira et al., 2009b). Prior to modelling, data normality had been tested by the Shapiro–Wilk test (SW) (Shapiro, Wilk, 1965) and considered normal at $p > 0.05$. Statistical analysis was carried out with Statistica 6.0. Statsoft Inc.

Interpolation methods

Interpolation methods can be different depending on their assumptions (from global to local perspective) and deterministic or stochastic nature (Luo et al., 2008; Erdogan, 2009).

Deterministic techniques are based on mathematical functions for interpolation and stochastic or geostatistical reliance on both statistical and mathematical methods that can be applied to create surfaces and access the uncertainty of the estimates. In this study, we selected and tested several interpolation methods in order to find the most accurate one for interpolating TN. The deterministic methods included the inverse distance to a weight (IDW), local polynomial interpolation (LP), global polynomial interpolation (GP), radial basis functions (RBF) – spline with tension (SPT), completely regularized spline (CRS), multiquadratic (MTQ), inverse multiquadratic (IMTQ) and thin plate spline (TPS) – and geostatistical methods such as ordinary kriging (OK) and simple kriging (SK). In all interpolations we applied a smooth factor of 0.5.

Inverse distance to a weight (IDW)

The IDW method is considered a quick but inexact interpolator and estimates the variables attributing more weight to closer points. The power of IDW controls the significance of known points on the interpolated values based on the distance from the output point. It is one of the simplest and popular methods and does not require prior information, namely, the variogram model to spatial prediction. It combines the proximity with the gradual change of the trend surface (Babak, Deutsch, 2009). It is calculated according to the following formula (Burrough, McDonnell, 2009):

$$\dot{Z}(S_0) = \sum_{i=1}^{N} \lambda_i Z(s_i), \tag{1}$$

where $\dot{Z}(S_0)$ is the predicted value for location (S_0), N is the number of measured points surrounding the prediction. λ_i are the weights allocated to each measured point, and $Z(s_i)$ is the observed value at the location (s_i). The weights are a function of the inverse distance and are calculated according to the formula:

$$\lambda_i = \frac{d_{i0}^{-p}}{\sum_{i=1}^{N} d_{i0}^{-p}}. \tag{2}$$

The power parameter (p) in this method of interpolation is the dependence of the surrounding points upon the interpolated value. When the distance (d) increases between the measured and the prediction points, the weight that the measured point has on the prediction is reduced (Burrough, McDonnell, 2009).

Local polynomial (LP)

LP is a moderately quick deterministic method which provides surfaces similar to those offered kriging methods. It combines polynomial methods and the moving average procedure (Luo et al., 2008; Yilmaz, 2008). This method can be of one, two or three orders. In the present study, we tested the first and second orders defined by the following formulas:

order 1

$$F(X, Y) = a + bX + cy, \tag{3}$$

order 2

$$F(X, Y) = a + bX + cY + dXY + eX^2 + f Y. \tag{4}$$

Radial base functions (RBF)

The RBF methods are exact and moderate, quick deterministic interpolators and more flexible than IDW. These methods are similar to those applied in geostatistical simulations, however, without variogram modeling. They do not make any assumption about the input data points (Smith et al., 2009). In the SPT method, the tension rules the flexibility of the surface according to the characteristics of the modelled phenomenon. This technique generates a less smooth surface with values more closely constrained by the sample data amplitude. In this work, we considered a tension of 0.1. In the SPT, the parameter defines the weight of tension: the higher the weight, the coarser the output surface. The spline function applies this formula for surface interpolation:

$$S(x, y) = T(x, y) + \sum_{j=i}^{N} \lambda_j R(r_j), \tag{5}$$

where $J = 1, 2, \ldots N$, N is the number of points, λ_j are coefficients found by solving a system of linear equations, r_j is the distance from the point (x, y) to the 3rd point. $T(x, y)$ and $R(r)$ are defined differently, depending on the selected RBF method. In the case of SPT,

$$T(x, y) = a1 \tag{6}$$

and

$$R(r) = -\frac{1}{2\pi\varphi^2}\left[\ln\left(\frac{r\varphi}{2}\right) + c + K_0(r\varphi)\right], \tag{7}$$

where ϕ^2 is the parameter entered at the command line, r is the distance between the point and the sample, K_0 is the modified Bessel function, and c is a constant equal to 0.57721 (Franke, 1982). CRS is a flexible method through the choice of the tension parameter which controls the characteristics of the interpolation function and the smoothing parameter. In this study, the tension parameter was 1.8567 (optimized in ArcGis and also applied in the other RBF methods). CRS is calculated according to the formula:

$$\phi_1(r) = \ln(cr/2)^2 + E_1(cr)^2 + \gamma, \tag{8}$$

where E_1 is the exponential integral function and γ is Euler's constant. Of all RBF methods, MQ is considered to be the most accurate for terrain modelling (Yang et al., 2004; Smith et al., 2009). It is calculated according to the formula

$$\varphi_1(r) = \sqrt{r^z + c^z}, \tag{9}$$

and for IMQ

$$\varphi_1(r) = \frac{1}{\sqrt{r^z + c^z}}, \tag{10}$$

where r is the vector of distances from the grid point, and c is the smoothing parameter. TPS is a method that ensures a smooth surface, together with continuous first derivate surfaces. It works by fitting a surface at each sample point, so the surface can be smother than if data were fitted exactly (Tait et al., 2005). The definition of this method is given by a linear combination (Luo et al., 2008) and is calculated according to the formula

$$z_p = w_i \phi (r_i), \tag{11}$$

where z_p is the estimated value for the surface at the grid point p, $\phi (r_i)$ is the RBF selected, with (r_i) being the radial distance from point p to the 1st data point. The weight w_i is estimated from the data points (Smith et al., 2009). In the present case, we selected TPS (ϕ) as RBF, hence

$$\phi = c^2 r^2 \ln (cr), \tag{12}$$

where c is the smoothing factor and r is the vector (Smith et al., 2009).

Kriging

Kriging is a moderately fast interpolator that takes into account both the distance and the degree of variation among known data points. This method is similar to IDW, because it uses a linear combination of weights at sampling points to estimate the values at unsampled points. One of the main advantages of kriging is analysis of the spatial correlation between the measured points, given by the variance that is computed as the average of the squared difference between two components of each data pair (Goovaerts, 2000; Chaplot et al., 2006; Luo et al., 2008, among others). The main advantage of kriging in comparison with other methods is the prediction of the spatial correlation among sampling points, calculated according to the formula:

$$\gamma(h) = \frac{1}{2N(h)} \sum_{i=1}^{N(h)} [Z(s_i) - Z(s_i) + h]^2, \tag{13}$$

where $N(h)$ is the number of data pairs within a given class of distance and direction. The semi-variance can be a function of distance and direction, and so it can identify the variable spatial dependence in a certain direction (anisotropy) (Luo et al., 2008). The computed semi-variogram is omnidirectional (assuming that the variability is identical in all directions). Kriging is expressed by the following formula (Borrough, McDonnell, 2009):

$$Z(s) = \mu(s) \sum(S), \tag{14}$$

where $Z(s)$ is the variable of interest, $\mu(s)$ is the deterministic trend, and $\varepsilon(S)$ is the random, autocorrelated errors.

In this work, we selected the OK and SK methods. OK is a univariate method and one of the most widespread procedures in GIS packages. Like the other kriging methods, it uses point or block computations, resulting in a smoothed surface and inexact interpolation. It assumes a constant but unknown average and estimates the average value as a constant on searching the neighbourhood (Goovaerts, 1999; Kumar et al., 2007; Smith et al., 2009). SK assumes that the data have a known, constant and mean value throughout the study area (Smith et al., 2009).

Assessment criteria for interpolation methods

The accuracy of interpolation methods is evaluated analyzing the errors produced by each model. In this study, we used the cross-validation procedure that compares the measured values with the estimated ones. The predicted values are obtained taking each observation in turn out of a sample and estimating from the remaining ones. The produced errors allow us to calculate in each method the mean error (ME) and the root mean square (RMSE). Normally, the ME should be close to 0. Among all the methods, the one with the lower RMSE is the most accurate for interpolating TN. This methodology was applied also in other studies (Serrano et al., 2003; Robinson, Metternicht, 2006; Gomez et al., 2008). The ME and RMSE are calculated according to the following formulas:

$$ME = \frac{1}{N} \sum_{i=1}^{n} \{z(x_i) - \hat{z}(x_i)\}, \tag{15}$$

$$RMSE = \sqrt{\frac{1}{N} \sum_{i=1}^{N} \{z(x_i) - \hat{z}(x_i)\}^2}, \tag{16}$$

where $z(x_i)$ is the observed value, $\hat{z}(x_i)$ is the predicted value, and N is the number of samples.

We calculated also the relative improvement in the percentage (RI%) by each method in relation to the best one according to the formula:

$$RI(\%) = \frac{(RMSE_{Best} - RMSE_{Current})}{RMSE_{Best}} * 100, \tag{17}$$

where $RMSE_{Best}$ is the minimum value of $RMSE$ and $RMSE_{Current}$ is the current model.

We observed also the relationship between the predicted and the observed values in each model and compared their mean values applying a t test for dependent samples significant at $p < 0.05$. Interpolation was performed with SURFER 8.0 (Golden software) and ArcGis 9.3 (ESRI software) for Windows.

RESULTS AND DISCUSSION

The descriptive statistics of TN in the study area are presented in Fig. 3. The mean of all samples was 1.796%, with a maximum of 2.640% and a minimum of 0.93%. Hence, we consider that the fire did not have negative implications in TN concentration. The spatial variability assessed by the CV(%) is not substantial, showing the absence of great and abrupt changes in ash TN across the study area. The variable

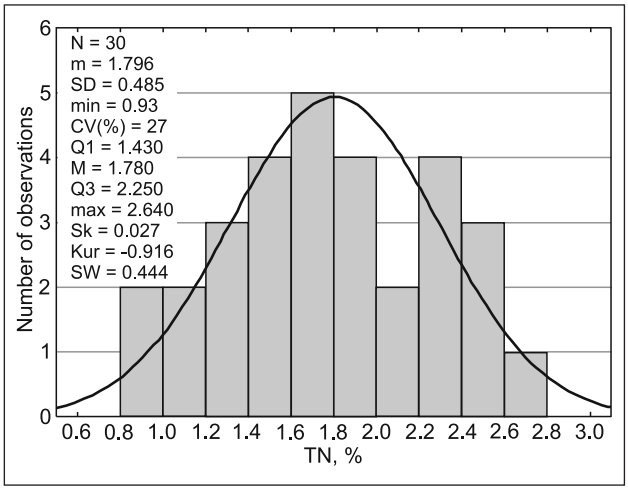

Fig. 3. Descriptive statistics and the dsitribution of ash TN content. Shapiro Wilk (SW) test

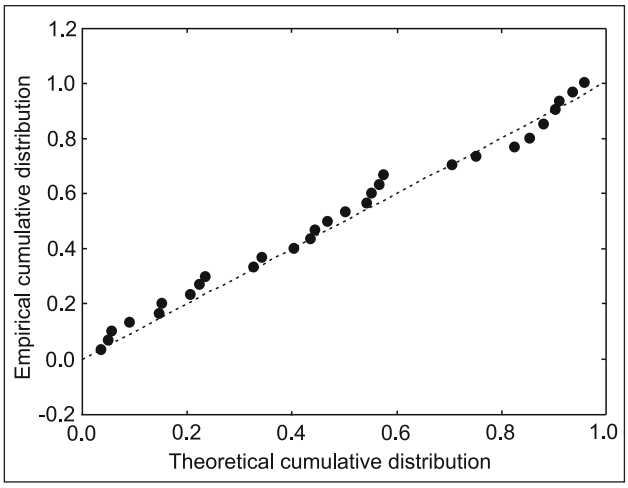

Fig. 4. P-P plot of ash TN concentration

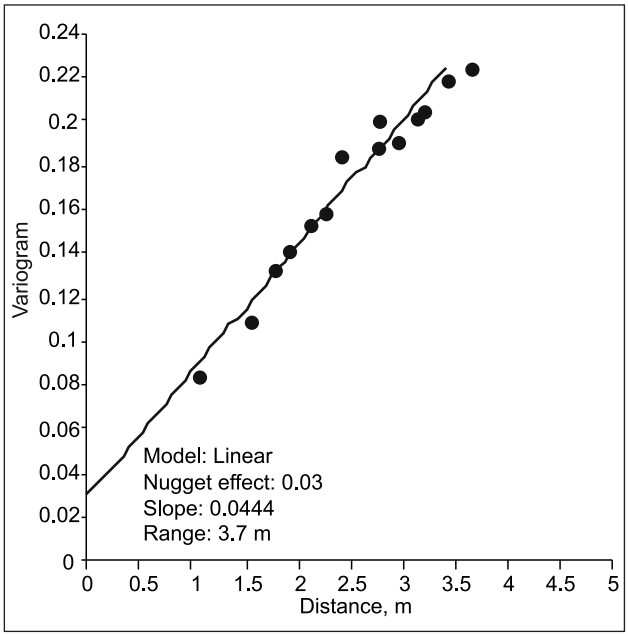

Fig. 5. Experimental isotropic variogram of ash TN content in Quinta do Conde plot

Table 1. **Correlation between ash color and $CaCO_3$ content. * Significant at p > 0.05**

Element	TN
Ash color	–0.44*
$CaCO_3$	–0.43*

follows the normal distribution because the p value of the SW test is higher than 0.05 and the points in the P–P plot are around the straight line (Fig. 4). This means that no transformation is needed prior to spatial modelling. Hence, the models were compiled applying the original data. TN concentration showed a significant negative correlation with the ash colour and $CaCO_3$ (Table 1). According to Pereira et al. (2009b) and Úbeda et al. (2009), ash with a higher Munsell CV and $CaCO_3$ content shows that samples were burned at a higher severity. A lower percentage of TN was concentrated where fire was more severe. A linear model was fitted to the experimental isotropic variogram; this means that the TN variability increases with the distance in all area of interest (Fig. 5). The model presents a reduced nugget effect, which shows that the sampling error is reduced, the sample density is adequate to reveal some spatial structures, and small-scale variances are not high. Hence the sample design is appropriate for studying TN, and we suppose that a good spatial structure will be observed on the interpolated map.

The highest ash TN concentrations were found in samples collected in some points at the north, northeast and the lowest in the central and eastern parts of the plot (Fig. 6). This punctual distribution gives an idea about TN distribution. To elucidate TN spatial distribution, we tested several interpolation methods in order to identify the best technique to predict ash TN in the unsampled points. The results of employing the interpolation methods are presented in Table 2. In general, the ME is reduced and close to 0, which means that the employed methods are unbiased. According to the results of this index, the IDW method in all tested powers, SK and LP1, subestimated, on average, the original values (i. e observed > predicted), contrary to the other methods tested in our study. The most accurate to interpolate TN was the MTQ (lower RMSE) and the worst was the IDW5 method (Table 2). In general, IDW methods were less precise to interpolate the variables with the higher errors in relation to the MTQ. In all cases they were always exceeded 14%. The RBF and geostatistical methods were most exact in predicting TN. In all tested techniques, the mean of the observed values was close to the estimated level, and the correlation between the observed and the predicted values was significant, especially in the RBF and geostatistical methods. Overall, excep LP2 and GP, the methods that were more accurate in interpolating TN overestimated the original values. On the contrary, the less precise methods, excluding LP1 and SK, subestimated TN. The LP methods were most and the GP and IDW1 least biased (Fig. 7).

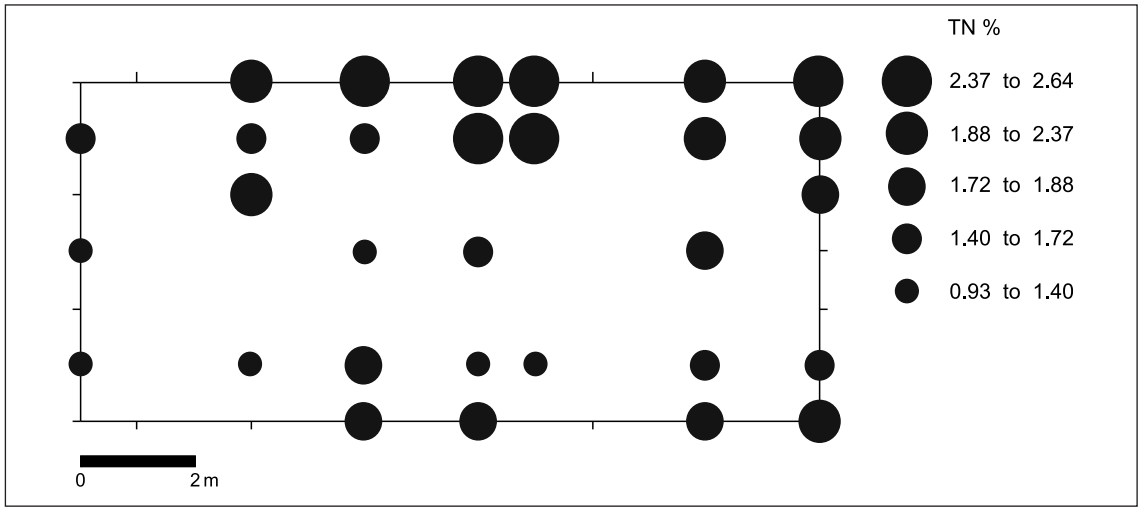

Fig. 6. Symbol map of TN distribution in the studied area

Table 2. **Summary statistics of the interpolation methods accuracy. Accuracy is assessed by the cross validation method. Minimum error (Min) and maximum error (Max) in each interpolation method: in bold the less biased and underlined the less accurate method. Differences between Obs vs Est. are significant at $p < 0.05$. Significant correlations at $p > 0.01$** and $p < 0.001$*****

Method	Min	Max	ME	RMSE	RI(%)	Obs *vs* Est	*r*
IDW 1	–0.6333	0.7732	0.002372	0.3816	18.80	0.9735	0.61***
IDW 2	–0.5789	0.7870	0.00621	0.3670	14.26	0.9280	0.64***
IDW 3	–0.6703	0.7541	0.009936	0.3842	19.61	0.8901	0.61***
IDW 4	–0.7772	0.8039	0.00876	0.4038	25.72	0.9077	0.58***
IDW 5	–0.8452	0.8544	0.01125	0.4174	29.95	0.8855	0.55**
LP 1	–0.7128	0.7293	0.02962	0.3427	6.69	0.6438	0.71***
LP 2	–0.9044	0.7709	–0.03342	0.3717	15.72	0.6304	0.70***
GP	–0.6704	0.7636	–0.002813	0.3677	14.48	0.9674	0.64***
SPT	–0.7090	0.5903	–0.01996	0.3394	5.67	0.7534	0.72***
CRS	–0.7758	0.5458	–0.01131	0.3361	4.64	0.8573	0.72***
MTQ	**–0.6553**	**0.5471**	**–0.01345**	**0.3212**	**–**	**0.8230**	**0.74*****
IMTQ	–0.7587	0.5450	–0.009545	0.3369	4.89	0.8797	0.72***
TPS	–0.7549	0.5070	–0.03208	0.3354	4.42	0.6087	0.75***
OK	–0.5286	0.5852	–0.01448	0.3339	3.95	0.8168	0.72***
SK	–0.5496	0.5454	0.00824	0.3531	9.93	0.9008	0.68***

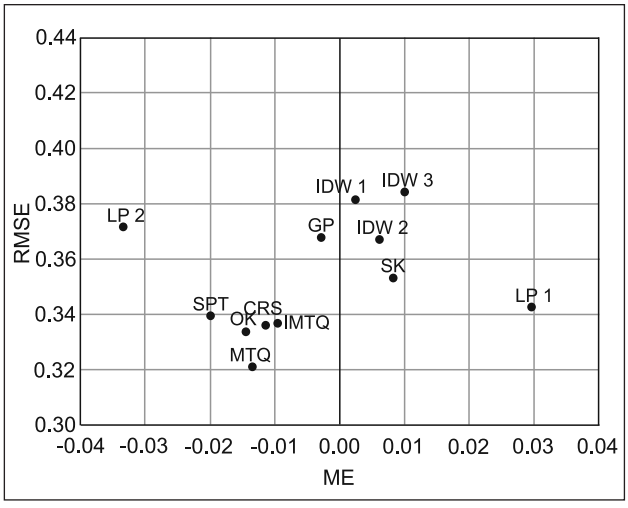

Fig. 7. Relation between ME and RMSE. Bold line shows 0 value

The interpolated maps with MTQ and IDW5 (the best and the worst of the considered techniques) are shown in Figs. 8 and 9. Generally, as described above, the major concentrations were observed in the northern and northeastern parts of the plot were this severity was more reduced, and in the southwestern area. Nevertheless, a careful analysis showed some spatial differences, especially in the northern and central parts of the plot where the IDW5 created "bull's eyes" around the data points (Fig. 9). This is a common characteristic of this method, also referred to in other studies (Smith et al., 2009; Sen, 2009). IDW methods are very sensitive to local variations. The influence of distant points is reduced with the increasing power, and this means that local factors have more influence on the estimated values. On the contrary, the RBF and geostatistical methods are less sensitive to local variations. Since the RBF and geostatistical methods are the best interpolates, ash TN distribution across

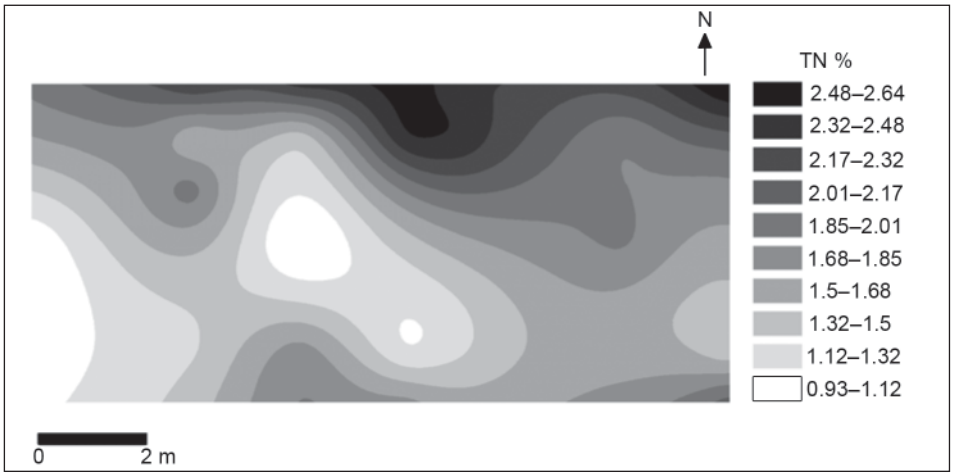

Fig. 8. Spatial distribution of TN according to MTQ interpolation method

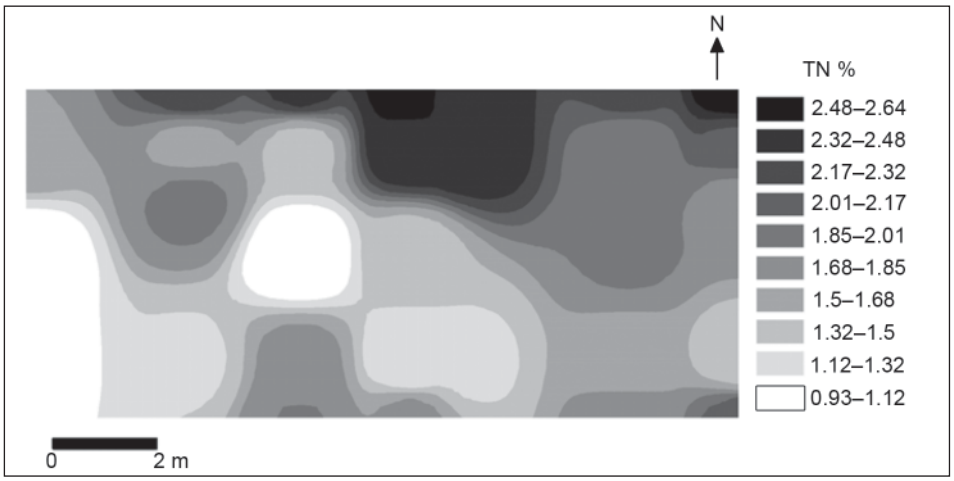

Fig. 9. Spatial distribution of TN according to IDW5 interpolation method

the plot was not influenced by local factors. This spatial pattern of fire severity effects on ash TN content is due to species distribution. The ash collected in the southwestern part of the plot was from *Pinus pinaster* and in the northeastern area from *Quercus suber*. Normally, litter from *Pinus* species is more vulnerable to fire temperatures than *Quercus* litter (Pereira et al., 2009c). Also, according to Pereira et al. (2009b), the ash produced in the eastern part of the plot was produced at higher temperatures. This means that TN concentration in ash depends also on the species affected. Also other variables, such as vegetation moisture during fire evolution, could influence fire severity. In the present case, the study area was not located on a steep slope. Thus, the topography seems had no great influence on fire behaviour and evolution across the plot as was the case in other places (Lorca, Úbeda, 2004; Pereira, Úbeda, 2010).

CONCLUSIONS

This study showed that the interpolation methods allow an accurate assessing of the spatial variation of ash TN. The variable distribution depends on fire severity and species distribution. Nevertheless, other factors, such as the content of TN in the litter before fire, fuel moisture, fuel patchiness, fuel distribution and density might be also important. These conditions were impossible to know after a wildfire, because we did not assess the study area conditions. This is only possible in prescribed fires that are planned in landscape management. Presently, we are monitoring the affected area, the responses of vegetation to fire and whether ash TN has implications in half-long term vegetation colonization of the burned area.

The major conclusions of this work are as follows:

1. The wildfire in the study plot had no coercive impact on TN content. The spatial variability across the study area was not substantial, and the variable showed a negative correlation with fire severity.

2. The TN isotropic experimental variogram showed a good structure and fitted with the linear model, which means that the variable variability increased in all the plot.

3. The major ash TN concentration was observed in the northeastern part of the plot and the lowest in the southwest.

4. The most accurate methods for interpolating TN was MTQ, and the worst was IDW5. In general, IDW methods were less precise in the variable interpolation. On the contrary, RBF and geostatistical methods were more accurate, which means that TN distribution depends on some spatial

patterns and does not exhibit small-scale variations. The effects of fire in TN distribution and concentration are mainly related to temperatures, species distribution and probably to vegetation moisture during fire evolution.

ACKNOWLEDGEMENTS

This study was supported by the Spanish Ministry of Science and Technology, project CGL2006-11107-C02-02/BOS "Evaluation of the quality of Mediterranean soils affected by fire in a middle and large term" and the European Regional Development Fund (FEDER). We are also thankful to Serveis Científico-Tècnics from the University of Barcelona.

Received 22 February 2010
Accepted 30 September 2010

References

1. Babak O., Deutsch C. 2009. Statistical approach to inverse distance interpolation. *Stochastic Environmental Research and Risk Assessment*. Vol. 23. P. 543–553.
2. Baeza M. J., Raventós J., Escarré A., Vallejo V. R. 2006. Fire risk and vegetation structural dynamics in Mediterranean shruband. *Plant Ecology*. Vol. 187. P. 189–201.
3. Bourennane H., Dère Ch., Lamy I., Cornu S., Baize D., van Oort F., King D. 2006. Enhancing spatial estimates of metal pollutants in raw wastewater irrigated fields using a topsoil organic carbon map predicted from aerial photography. *Science of Total Environment*. Vol. 361. P. 229–248.
4. Burrough P. A., McDonnell R. A. 2009. *Principles of Geographical Information Systems*. New York: Oxford University Press. P. 356.
5. Chaplot V., Darboux F., Bourennane H., Leguédois S., Silvera N., Phachomphon K. 2006. Accurancy of interpolation techniques for derivation of digital models in relation to landform types and data sensivity. *Geomorphology*. Vol. 77. P. 126–141.
6. Crimmins M. A. 2006. Synoptic climatology of extreme fire weather conditions across southwest United States. *International Journal of Climatology*. Vol. 26. P. 1001–1016.
7. DeBano L. F. 1981. *Water-repellent Soils: A State-of-Art*. General Technical Report PSW 46. Berkley, CA: USDA Forest Service.
8. DeBano L. F., Neary D. G., Ffolliott P. F. 1998. *Fire Effects on Ecosystems*. New York: John Wiley & Sons. P. 352.
9. Diodato N., Ceccarelli M. 2005. Geographical Information Systems and Geostatistics for modelling radioactivity contaminated land areas. *Natural Hazards*. Vol. 35. P. 229–242.
10. Erdogan S. 2009. A comparison of interpolation methods for producing digital elevation models at the field scale. *Earth Surface and Landforms*. Vol. 34. P. 366–376.
11. Erxleben J., Elder K., Davies R. 2002. Comparison of spatial interpolation methods for estimating snow distributions in the Colorado Rocky Mountains. *Hydrological Processes*. Vol. 16. P. 3627–3649.
12. Franke R. 1982. Smooth interpolation of scattered data by local thin plate splines. *Computation & Mathematics with Applications*. Vol. 8. P. 237–281.
13. Gomez C., Viscarra Rossel R. A., McBratney A. B. 2008. Soil organic carbon prediction by hyperspectral remote sensing and field vis – NIR spectroscopy: An Australian case. *Geoderma*. Vol. 146. P. 403–411.
14. Goovaerts P. 1999. Geostatistics in soil science: state of art and perspectives. *Geoderma*. Vol. 89. P. 1–45.
15. Goovaerts P. 2000. Geostatistical approaches for incorporating elevation into spatial interpolation of rainfall. *Journal of Hydrology*. Vol. 228. P. 113–129.
16. Kumar A., Maroju S., Bhat A. 2007. Application of ArcGIS geostatistical analyst for interpolating environmental data from observations. *Environmental Progress*. Vol. 26. P. 220–225.
17. Lorca M., Úbeda X. 2004. The effects of a prescribed burning in the soil (Prades mountains, Northeast Iberian Peninsula). *Geophysical Research Abstracts*. Vol. 6.
18. Luo W., Taylor M. C., Parker S. R. 2008. A comparison of spatial interpolation methods to estimate wind speed surfaces using irregularity distributed data from England and Wales. *International Journal of Climatology*. Vol. 28. P. 946–959.
19. Maingi J., Henry M. C. 2007. Factors influencing wildfire occurence and distribution in eastern Kentucky, USA. *International Journal of Wildland Fire*. Vol. 16. P. 23–33.
20. Mataix-Solera J., Cerdà A. 2009. Forest fires in Spain. Terrestrial ecosystems and soils. In: Cerdà A., Mataix-Solera J. (eds.). *Forest Fires Effects on Soil in Spain*. *State of the Art Viewed by the Spanish Scientists*. P. 25–55.
21. Munsell. 1975. *Soil Color Chart. Baltimore*. U.S. Department of Agriculture.
22. Pereira P., Úbeda X. 2010. Spatial variation of heavy metals released from ashes after a wildfire. *Journal of Environmental Engineering and Landscape Management*. Vol. 18(1). P. 13–22.
23. Pereira P., Úbeda X., Martin D., Miguel A. 2009b. Ash color and $CaCO_3$ as methods of burning severity classification. In: Jordán A., Zavala L. M., de la Rosa J., Knicker H., Gonzalez-Perez J. A., Gonzalez-Villa F. A. *II International Meeting of Fire Effects on Soils (Fuegored)*. Sevilla-Cortegana, Huelva.
24. Pereira P., Úbeda X., Martin D. A. 2009c. Application of a clusters analysis to the relationship between fire temperature and solutes release in some Mediterranean species. *Silva Lusitana.* Vol. 17. P. 39–50.
25. Pereira P., Úbeda X., Outeiro L., Martin D. A. 2009a. Factor analysis applied to fire temperature effects on water quality. In: Gomez E. & Alvarez K. (eds.). *Forest Fires: Detection, Suppression and Prevention*. Series Natural Disaster Research, Prediction and Mitigation, Chapter 9. P. 273–285.
26. Pereira P., Úbeda X., Martin D. A., Mataix-Solera J., Guerrero C. 2010. Effects of a low severity prescribed fire on water-soluble elements in ash from Cork Oak (*Quercus suber*) forest located in the northeast of the Iberian Peninsula. *Environmental Research* (in press) DOI: 10.1016/J.ENV.RES.2010.09.002

27. Robinson T. P., Metternicht G. 2006. Testing performance of spatial interpolation techniques for mapping soil properties. *Computers and Electronics in Agriculture*. Vol. 50. P. 97–108.
28. Sen Z. 2009. *Spatial modelling principles in Earth Sciences*. New York: Springer. P. 351.
29. Serrano S. M., Saz-Sanchez M. A., Cuadrat J. M. 2003. Comparative analysis of interpolation methods in the middle Ebro Valley (Spain): application to annual precipitation and temperature. *Climate Research*. Vol. 24. P. 161–180.
30. Shapiro S., Wilk M. 1965. An analysis of variance test for normality. *Biometrika*. Vol. 52. P. 591–611.
31. Smith M. J., Goodchild M. F., Longley P. A. 2009. *Geospatial Analysis. A Comprehensive Guide to Principles Techniques and Software Tools*. Leicester: Troubador Publishing. P. 394.
32. Tait A., Henderson R., Turner R., Zheng X. 2006. Thin plate smoothing spline interpolation of daily rainfall for New Zealand using a climatological rainfall surface. *International Journal of Climatology*. Vol. 26. P. 2097–2115.
33. Úbeda X., Lorca M., Outeiro L. R., Bernia S., Castellnou M. 2005. Effects of a prescribed fire on soil quality in Mediterranean grassland. *International Journal of Wildland Fire*. Vol. 14. P. 379–384.
34. Úbeda X., Pereira P., Outeiro L., Martin D. A. 2009. Effects of fire temperature on the physical and chemical characteristics of the ash from two plots of cork oak (*Quercus suber*). *Land Degradation and Development*. Vol. 20. P. 589–608.
35. Viegas D. X. 2004. On the existence of a steady state regime for slope and wind driven fires. *International Journal of Wildland Fire*. Vol. 13. P. 101–117.
36. Webster R., Oliver M. A. 2007. *Geostatistics for Environmental Scientists*.. 2nd edn. Wiley. P. 330.
37. Yang C. S., Kao S. P., Lee F. B., Hung P. S. 2004. Twelve different interpolation methods: a case study of surfer 8.0. *ISPRS*. P. 778–783.
38. Yilmaz H. M. 2009. The effect of interpolation methods in surface definition: an experimental study. *Earth Surface and Landforms*. Vol. 32. P. 1346–1361.
39. Zhang C., McGrath D. 2004. Geostatistical and GIS analysis on soil organic carbon concentrations in grassland of southeastern from two different periods. *Geoderma*. Vol. 119. P. 261–275.

Paulo Pereira, Xavier Úbeda, Edita Baltrėnaitė

BENDROJO AZOTO PELENUOSE PO GAISRO TERITORINIS PASISKIRSTYMAS: MAŽOS TERITORIJOS ANALIZĖ

S a n t r a u k a

Gaisro atveju azotas (A) yra viena jautriausių maisto medžiagų dėl žemos garavimo temperatūros. Jo koncentracijos kitimas priklauso nuo gaisro poveikio stiprumo dėl biofizikinių salygų ir yra labai heterogeniškas gaisro paveiktame skirtingame kraštovaizdyje. Todėl gaisro poveikis A pokyčiams gali būti labai įvairus. Azoto koncentracijos gali kisti ir nedideliais atstumais, todėl sunkiau globaliai vertinti gaisro poveikį kraštovaizdžiui.

Šio tyrimo tikslas – įvertinti bendrojo azoto (BA) pelenuose pasiskirstymą gaisro paveiktoje teritorijoje ir palyginti kelis interpoliacijos metodus, siekiant nustatyti tiksliausią iš jų šio tyrimo atveju. Darbe palyginti 8 interpoliacijos metodai – *inverse distance to a weight (IDW)* su svorio koeficientais 1, 2, 3, 4 ir 5; *local polynomial (LP)* su svorio vertėmis 1 ir 2; *global polynomial (GP)*; *Radial basis functions (RBF) – spline with tension (SPT)*; *completely regularized spline (CRS)*, *multiquadratic (MTQ)*, *inverse multiquadratic (IMTQ)* ir *thin plate spline (TPS)* – ir geostatistiniai metodai – *ordinary kriging (OK)* ir *simple kriging (SK)*. Nustatyta, kad BA koncentracija pelenuose yra neigiamai proporcinga gaisro poveikio stiprumui, o jos vertės nagrinėjamame plote pasiskirstė tolygiai. Linijinis modelis buvo tinkamiausias, vadinasi, galima teigti, kad BA koncentracijos pelenuose pokytis didėjo nagrinėjamame plote. Didžiausia BA koncentracija aptikta šiaurrytinėje dalyje, o mažiausia – pietvakarinėje. Iš visų taikytų metodų *MTQ* buvo įvertintas geriausiai, o *IDW5* – mažiau tiksliai įvertinantis BA koncentracijos pelenuose pokyčius. Bendruoju atveju *RBF* ir geostatistiniai metodai, palyginti su *IDW*, yra tikslesni. Tokiu atveju BA koncentracijos pelenuose pasiskirstymui būdingi specialūs bruožai, tačiau nebūdingi staigūs kitimai. Kintamojo pasiskirstymas priklauso nuo medžių rūšies, gaisro temperatūros ir galbūt gaisro metu kintančios augalijos drėgmės.

Raktažodžiai: gaisro poveikio stiprumas, biofizikinės sąlygos, bendrojo azoto koncentracija pelenuose, interpoliacijos metodai